

## Energetics and Electronic Structures of Encapsulated C<sub>60</sub> in a Carbon Nanotube

Susumu Okada,<sup>1</sup> Susumu Saito,<sup>2</sup> and Atsushi Oshiyama<sup>3</sup>

<sup>1</sup>*Institute of Material Science, University of Tsukuba, Tennodai, Tsukuba 305-8573, Japan*

<sup>2</sup>*Department of Physics, Tokyo Institute of Technology, 2-12-1 Oh-okayama, Meguro-ku, Tokyo 152-8551, Japan*

<sup>3</sup>*Institute of Physics, University of Tsukuba, Tennodai, Tsukuba 305-8571, Japan*

(Received 12 January 2001)

We report total-energy electronic structure calculations that provide energetics of encapsulation of C<sub>60</sub> in the carbon nanotube and electronic structures of the resulting carbon peapods. We find that the encapsulating process is exothermic for the (10, 10) nanotube, whereas the processes are endothermic for the (8, 8) and (9, 9) nanotubes, indicative that the minimum radius of the nanotube for the encapsulation is 6.4 Å. We also find that the C<sub>60</sub>@(10, 10) is a metal with multicarriers each of which distributes either along the nanotube or on the C<sub>60</sub> chain. This unusual feature is due to the nearly free electron state that is inherent to hierarchical solids with sufficient space inside.

DOI: 10.1103/PhysRevLett.86.3835

PACS numbers: 71.20.Tx, 73.20.At, 73.22.-f

Discoveries of fullerenes [1] and carbon nanotubes [2] have triggered a great expansion of both theoretical and experimental research on the materials. Local atomic structures of these new materials are not new but similar to that of graphite: The  $sp^2$  hybridization renders a carbon atom threefold coordinated with its neighbors. Novelty lies in the global atomic network of the materials, however: The fullerene has a closed network with zero dimension, whereas the nanotube has a one-dimensional tubule network. This network topology decisively affects electronic properties of the materials [3–6], in a range from insulators to metals, and to superconductors under certain conditions [7], in their solid forms [8,9]. In the solid forms, fullerenes or nanotubes are constituent units which are weakly bound in some cases (the fcc C<sub>60</sub>, the nanotube bundle [10], etc.) and strongly bonded in another (C<sub>60</sub> polymers [11,12]). Therefore fullerenes and nanotubes may be regarded as natural super atoms which could be self-organized to become a unique class of solids with structural hierarchy. One of the prominent features of the hierarchical solids is the space between or within the constituent units. The space generates peculiar electron states called nearly free electron (NFE) states [13,14] whose amplitudes are not near atomic sites but in the spacious region of the hierarchical solids.

Recently, fullerenes *and* tubes were assembled: Transmission electron microscopy clearly shows that fullerenes (C<sub>60</sub>, C<sub>70</sub>, and C<sub>80</sub>) are aligned in a chain and encapsulated in carbon nanotubes [15–20]. This eccentric structure, occasionally called a carbon peapod, is an ultimate version of the hierarchical solids consisting of fullerenes and nanotubes and exhibits unprecedented properties that we will discuss in this Letter.

We here report total-energy electronic-structure calculations performed for one-dimensional chains of C<sub>60</sub> which are encapsulated in nanotubes. We take ( $n, n$ ) nanotubes ( $n = 8, 9, \text{ and } 10$ ) as representatives and clarify salient characteristics of carbon peapods. We find that electronic structure of the peapod is not a simple sum of those of

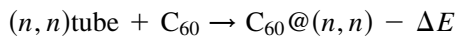
fullerenes and nanotubes. In the (10, 10) peapod, a NFE state located between the tube and the fullerenes is found to work as an acceptor state, controlling relative locations of electronic levels and the Fermi energy  $\epsilon_F$ . As a result, the (10, 10) peapod is a metal with multicarriers each of which is distributed either on the nanotube or on the chain of the fullerenes. We also find that the incorporation of C<sub>60</sub> into the (10, 10) tube is exothermic: The energy gain in forming the peapod from C<sub>60</sub> plus the empty (10, 10) tube is 0.51 eV per C<sub>60</sub>. On the other hand, the incorporation of C<sub>60</sub> in the (8, 8) and (9, 9) nanotubes is found to be endothermic due to large structural deformation of both fullerenes and nanotubes upon incorporation. This indicates that the smallest radius of the nanotube which is capable of encapsulating C<sub>60</sub> is about 6.4 Å (see below).

All calculations have been performed using the local-density approximation (LDA) in the density-functional theory [21,22]. For the exchange-correlation energy among electrons, we use a functional form [23] fitted to the Monte Carlo results for the homogeneous electron gas [24]. Norm-conserving pseudopotentials generated by using the Troullier-Martins scheme are adopted to describe the electron-ion interaction [25,26]. In constructing the pseudopotentials, core radii adopted for C 2s and 2p states are both 1.5 bohr. The valence wave functions are expanded by the plane-wave basis set with a cutoff energy of 50 Ry which is known to give enough convergence of total energy to discuss the relative stability of various carbon phases [25]. We adopt a supercell model in which a peapod is placed with its nanotube wall being separated by 6.5 Å from another wall of an adjacent peapod. The conjugate-gradient minimization scheme is utilized both for the electronic-structure calculation and for the geometry optimization [27]. In the geometry optimization, we impose a commensurability condition between the one-dimensional periodicity of the atomic arrangements in the nanotube and that of the chain of C<sub>60</sub>s. Consequently, the lattice parameter  $c$  become 9.824 Å along the tube direction which corresponds to the quadruple of the

periodicity of the armchair nanotube. Integration over one-dimensional Brillouin zone is carried out using the two  $k$  points.

Figure 1 shows total-energy minimized atomic geometries of  $C_{60}$  encapsulated in the (8, 8), (9, 9), and (10, 10) nanotubes. In the (10, 10) peapod,  $C_{60}@ (10, 10)$ ,  $C_{60}$  inside and the nanotube outside almost keep their original shapes before encapsulation. The calculated distance between the wall of the (10, 10) nanotube and the nearest atom of  $C_{60}$  is 3.31 Å which is close to the interlayer distance of graphite (3.34 Å) or the inter- $C_{60}$  distance in the fcc  $C_{60}$ . On the other hand, the space provided by the (9, 9) and the (8, 8) nanotube is insufficient for  $C_{60}$ : Both the tube and the fullerenes are substantially distorted in the (9, 9) peapod,  $C_{60}@ (9, 9)$ , and in the (8, 8) peapod,  $C_{60}@ (8, 8)$ . The fullerenes inside are elongated along the tube direction and the tube silhouette itself becomes undulating. The difference in diameter between the thinnest and thickest parts in the (8, 8) peapod is 0.6 Å which is visible in Fig. 1(c). The calculated distances between the wall of the nanotubes and the nearest atoms of  $C_{60}$  are 2.75 and 2.45 Å in  $C_{60}@ (9, 9)$  and  $C_{60}@ (8, 8)$ , respectively.

These characteristics in the geometry are reflected in total energies of the peapods. The energy difference in the reaction,



is shown in Fig. 2. The reaction is exothermic for  $n = 10$  and endothermic for  $n = 9$  and 8:  $\Delta E$  are  $-0.51$  eV, 0.27 eV, and 15.19 eV for  $n = 10, 9$ , and 8, respectively. It is thus concluded that the (10, 10) nanotube is capable of accommodating  $C_{60}$  inside and the encapsulation is energetically favorable. Further, once  $C_{60}$  is trapped inside, the escaping process is unlikely even if ends of the tube are open or there are holes on sidewalls since the escaping barrier is at least more than 0.51 eV. On the other hand, it costs substantial energy for the (8, 8) and (9, 9) nanotubes

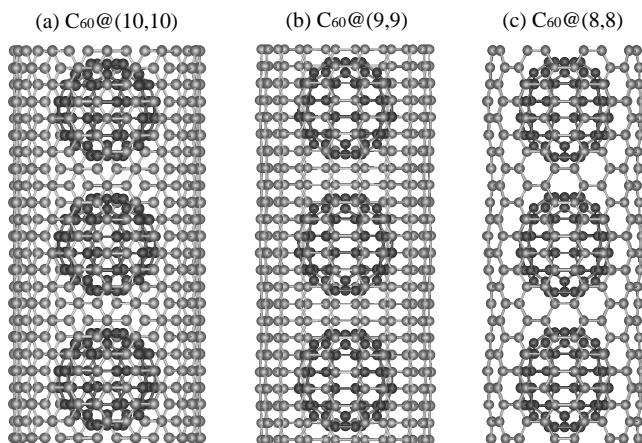


FIG. 1. Total-energy optimized geometries of  $C_{60}$  encapsulated in (a) the (10, 10), (b) the (9, 9), and (c) the (8, 8) nanotubes. Distances between  $C_{60}$ s are 3.14, 3.15, and 2.45 Å, for (10, 10), (9, 9), and (8, 8) peapods, respectively.

to accommodate  $C_{60}$ . The energy cost may be reduced when we release the commensurability condition on the periodicity. Yet we provisionally conclude that the encapsulation process is unlikely for the (8, 8) nanotube. We here consider only armchair nanotubes. There are indeed chiral nanotubes with a variety of radii. From the present calculations it is clear that the tube- $C_{60}$  interaction in the stable peapod is not due to chemical bonds. Hence from Fig. 2, we argue that the minimum radius of the nanotube for the encapsulation of  $C_{60}$  is about 6.4 Å.

Electronic energy bands for the (10, 10), the (9, 9), and the (8, 8) peapods are shown in Figs. 3(a), 3(b), and 3(c), respectively. In an isolated  $C_{60}$ , there are the fivefold degenerate highest occupied  $h_u$  state and the threefold degenerate lowest unoccupied  $t_{1u}$  state. In the fcc  $C_{60}$ , both  $h_u$  and  $t_{1u}$  show the dispersion of  $\sim 0.6$  eV [3] and become valence and conduction bands, respectively. The energy gap remains finite and is about 1 eV [3]. As for the  $(n, n)$  nanotube, there are two energy bands near Fermi energy, and the two bands cross with  $\epsilon_F$  at  $k \simeq 2\pi/3$  of Brillouin zone [5]. Therefore it may be expected in  $C_{60}@ (n, n)$  that the two bands originated from the nanotube cross  $\epsilon_F$  and are located in the gap of  $C_{60}$ , and that the peapod is metallic [28].

Yet Fig. 3(a) clearly shows a new feature that is missing in the discussion above. Four bands cross the Fermi level in the (10, 10) peapod,  $C_{60}@ (10, 10)$ : Two of them have large linear dispersion, keeping the character of the  $\pi$  orbitals on the nanotube, whereas the other two have less dispersion similar to the  $\pi$  state on the  $C_{60}$  chain. It is found that the latter two bands keep the character of the  $t_{1u}$  state of  $C_{60}$ . The (10, 10) peapod is thus a metal with

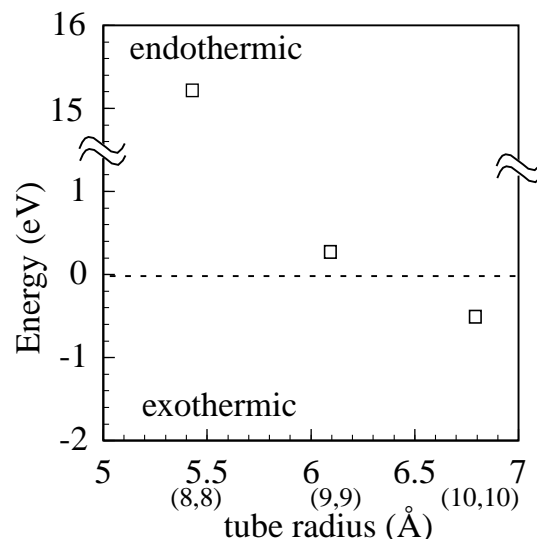


FIG. 2. Reaction energies  $\Delta E$  (see text) per  $C_{60}$  in the encapsulation reaction for the (8, 8), (9, 9), and (10, 10) nanotubes. The energy approaches zero with increasing radius when we place  $C_{60}$  at the center of the tube. A simple linear interpolation shows that the reaction energy crosses zero at the tube radius of 6.4 Å.

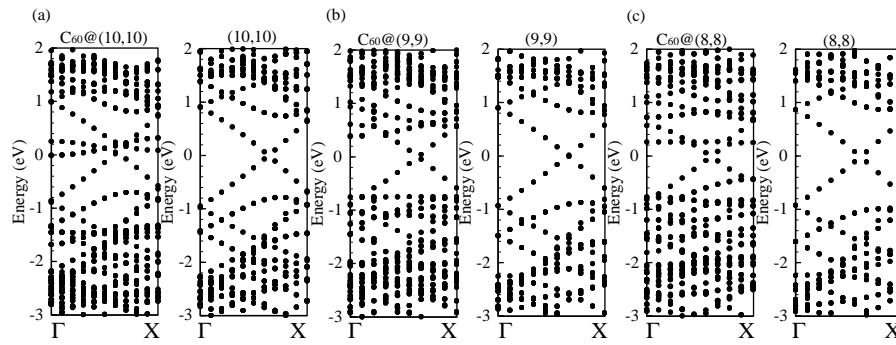


FIG. 3. Energy band structures of encapsulated  $C_{60}@n,n$  and of isolated  $(n,n)$  nanotube. (a)  $n = 10$ , (b)  $n = 9$ , and (c)  $n = 8$ . Energies are measured from the Fermi level energy  $\varepsilon_F$ .

multicarriers, each of which distributes mainly either on the tube or on the  $C_{60}$  chain. On the other hand, energy bands of the (8, 8) and (9, 9) peapods do not exhibit such a feature [Figs. 3(b) and 3(c)]. Only two bands which have  $\pi$  character of the nanotube cross the Fermi level. In the (8, 8) peapod, structural distortion is so substantial that the resulting energy bands are not the sum of electron states of the constituents before the encapsulation plus the effects of the atomic distortion. However, the energy bands of the (8, 8) and (9, 9) peapods are understandable in terms of the electron states of the constituents before the encapsulation plus the effects of the atomic distortion. The (8, 8) and (9, 9) peapods are metals and, in sharp contrast to the (10, 10) peapod, the charge density at  $\varepsilon_F$  distributes only along the walls of the nanotubes.

The difference in energy bands between the (10, 10) peapod and the (8, 8) and (9, 9) peapods is attributed to the space inherent to the hierarchical solids, as we explain below. Figure 4(a) shows electron charge density of the (10, 10) peapod,  $C_{60}@10,10$ . We observe the low charge density between the  $C_{60}$  and the nanotube, which indicates that the constituent units are bound weakly as in the fcc  $C_{60}$  or in the nanotube bundle. The peapod,  $C_{60}@n,n$ , has certainly the hybrid bonding networks with mixed dimensionality. When we carefully examine the charge density, an important role of the NFE state is elucidated. In Fig. 4(a), the difference between the charge density of  $C_{60}@10,10$  and the sum of the charge densities of the nanotube and of the  $C_{60}$  chain is also shown. It is clear that electrons are transferred mainly from  $\pi$  orbitals of the nanotube to the space between the tube and  $C_{60}$ : The distribution of the electron rich region ( $\Delta\rho^-$ ) is similar to that of the NFE state. The energy level of the NFE state is generally located at a couple of eV above  $\varepsilon_F$  in nanotubes [14]. This state is still above  $\varepsilon_F$  even in  $C_{60}@10,10$ . The hybridization between the NFE state and the  $\pi$  and  $\sigma$  orbitals of  $C_{60}$  is, however, substantially induced upon encapsulation of the fullerenes in the tube. The hybridization occurs not with particular states of an isolated  $C_{60}$  but with most  $\pi$  and  $\sigma$  orbitals. Analysis of wave functions of the Kohn-Sham orbitals in a range of  $-4 \sim 3$  eV in  $C_{60}@10,10$  confirms this situation. As a result of this, most of the electron states originated

in  $p$  orbitals of  $C_{60}$  shift downward upon encapsulation. These downward shifts of  $C_{60}$  states render the peapod,  $C_{60}@10,10$ , a metallic system with different characters of multicarriers, as is shown in Fig. 3(a). The electronic structure of the  $C_{60}@10,10$  obtained by using the generalized tight-binding model does not show these downward shifts [26]. Although the model used reproduces the LDA  $\sigma$  and  $\pi$  states very well, it cannot describe the NFE state.

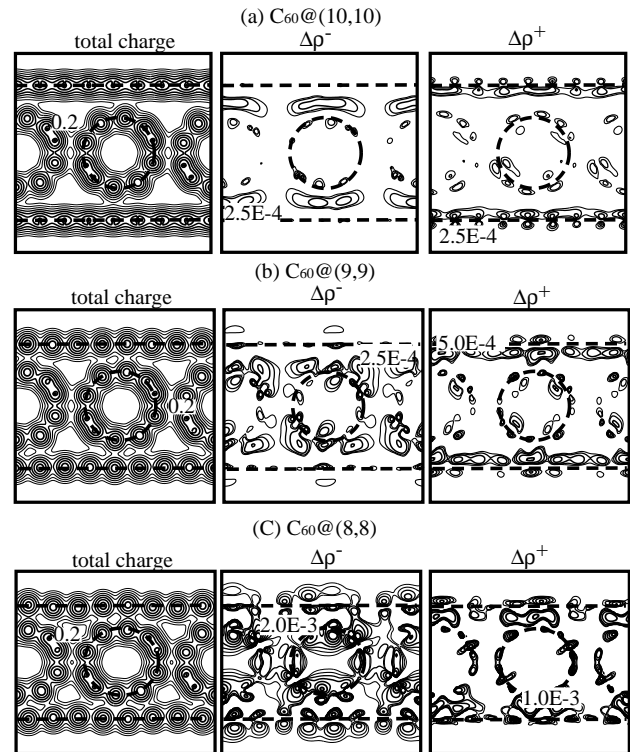


FIG. 4. Contour plots of the total valence charge density of  $C_{60}@n,n$ . (a)  $n = 10$ , (b)  $n = 9$ , and (c)  $n = 8$ . The contour plot of more negatively charged (electron rich) area,  $\Delta\rho^-$ , and that of the more positively charged,  $\Delta\rho^+$ , than a simple sum of two self-consistent charge densities of the tubes and  $C_{60}$  are also shown. Each contour represents twice (or half) the density of the adjacent contour lines. The values shown in figures are in units of  $e/(\text{a.u.})^3$ .

The charge densities of the thinner peapods are quite different from that of  $C_{60}@ (10, 10)$  [Figs. 4(b) and 4(c)]. We certainly observe charge redistribution upon encapsulation: Electrons are transferred from  $\pi$  orbitals of the nanotube to the spacious region inside the tube and around the fullerenes. Yet no single specific state such as the NFE state is responsible for this charge transfer. This is because the space between the constituents in the (9, 9) and (8, 8) peapods is not sufficient to generate the NFE state located at a couple of eV near  $\varepsilon_F$ : Probably the NFE state is above the vacuum level. In this case, relative location of electron states originating from the nanotube and from the  $C_{60}$  is essentially unchanged by the encapsulation. The resulting energy bands are thus given in Figs. 3(b) and 3(c). When the NFE state appears in a suitable energy range as in  $C_{60}@ (10, 10)$ , it selectively hybridizes with  $p$  orbitals of  $C_{60}$  and hereby produces the interesting variation of energy bands at  $\varepsilon_F$ . The space inherent to the hierarchical solids thus controls the electron states of  $C_{60}@ (n, n)$ .

One-dimensional conductors are generally expected to show the metal-insulator transition associated with lattice distortion (Peierls transition [29]). An earlier theoretical calculation [30] shows that the nanotube itself is robust against the Peierls instability. It is thus expected that the metallic nature of  $C_{60}@ (8, 8)$  and  $C_{60}@ (9, 9)$  is preserved. In  $C_{60}@ (10, 10)$ , however, some carriers are distributed along the chain of  $C_{60}$ , leading to displacements of  $C_{60}$  molecules. The calculated energy bands of  $C_{60}@ (10, 10)$  near  $\varepsilon_F$  in Fig. 3(a) show that the filling is incommensurate: Thus incommensurate charge density waves are generally expected. Since the space is decisive to control energy bands, however, we expect that the filling is sensitive to the radius of the encapsulating nanotube. Hence displacements of fullerenes in peapods may exhibit variation depending on the tube radii and, in other cases, on sizes of fullerenes. Some experimental images by the transmission electron microscope [15–18] indeed show dimerization of  $C_{60}$  molecules in the peapods. This might be due to the Peierls-type transition. Even in this case,  $C_{60}@ (10, 10)$  is still a metal but the state along the wall of the nanotube is responsible for the metallic nature.

In summary, we have found the peapod  $C_{60}@ (10, 10)$  is stable and the reaction of the encapsulation of  $C_{60}$  in (10, 10) nanotube is exothermic with the energy gain of 0.51 eV. We have also evaluated that the minimum radius of the nanotube which is capable of encapsulating  $C_{60}$  is 6.4 Å. We have also found that the peapod  $C_{60}@ (10, 10)$  is a metal with multicarriers each of which distributes either along the nanotube or on the fullerenes. This unusual electronic structure is due to the space which generates the nearly free-electron states inherent to the hierarchical solids.

We thank Dr. H. Kataura for discussions. Computations were done at ISSP, University of Tokyo and at RCCS,

Okazaki National Institute. This work was supported in part by JSPS under Contract No. RFTF96P00203 and by Grant-in-Aid for Scientific Research No. 11740219 and “Fullerenes and Nanotubes.”

- 
- [1] H. W. Kroto *et al.*, *Nature (London)* **318**, 162 (1985); W. Krätschmer *et al.*, *Nature (London)* **347**, 354 (1990).
  - [2] S. Iijima, *Nature (London)* **354**, 56 (1991).
  - [3] S. Saito and A. Oshiyama, *Phys. Rev. Lett.* **66**, 2637 (1991).
  - [4] M. B. Jost *et al.*, *Phys. Rev. B* **44**, 1966 (1991).
  - [5] N. Hamada, S. Sawada, and A. Oshiyama, *Phys. Rev. Lett.* **68**, 1579 (1992).
  - [6] R. Saito *et al.*, *Appl. Phys. Lett.* **60**, 2204 (1992).
  - [7] A. F. Hebard *et al.*, *Nature (London)* **350**, 632 (1991).
  - [8] For a review of earlier works on fullerenes, see A. Oshiyama *et al.*, *J. Phys. Chem. Solids* **53**, 1457 (1992).
  - [9] See, for instance, R. Saito, G. Dresselhaus, and M. S. Dresselhaus, *Physical Properties of Carbon Nanotubes* (Imperial College Press, London, 1998).
  - [10] A. Thess *et al.*, *Science* **273**, 483 (1996).
  - [11] Y. Iwasa *et al.*, *Science* **264**, 1570 (1995); S. Okada and S. Saito, *Phys. Rev. B* **59**, 1930 (1999).
  - [12] S. Okada, S. Saito, and A. Oshiyama, *Phys. Rev. Lett.* **83**, 1986 (1999).
  - [13] Y. Miyamoto *et al.*, *Phys. Rev. Lett.* **74**, 2993 (1995).
  - [14] S. Okada, A. Oshiyama, and S. Saito, *Phys. Rev. B* **62**, 7634 (2000).
  - [15] B. W. Smith, M. Monthieux, and D. E. Luzzi, *Nature (London)* **396**, 323 (1998).
  - [16] B. Bouteaux *et al.*, *Chem. Phys. Lett.* **310**, 21 (1999).
  - [17] B. W. Smith, M. Monthieux, and D. E. Luzzi, *Chem. Phys. Lett.* **315**, 31 (1999).
  - [18] J. Sloan *et al.*, *Chem. Phys. Lett.* **316**, 191 (2000).
  - [19] H. Kataura *et al.*, *Synth. Met.* (to be published).
  - [20] K. Hirahara *et al.*, *Phys. Rev. Lett.* **85**, 5384 (2000).
  - [21] P. Hohenberg and W. Kohn, *Phys. Rev.* **136**, B864 (1964).
  - [22] W. Kohn and L. J. Sham, *Phys. Rev.* **140**, A1133 (1965).
  - [23] J. P. Perdew and A. Zunger, *Phys. Rev. B* **23**, 5048 (1981).
  - [24] D. M. Ceperley and B. J. Alder, *Phys. Rev. Lett.* **45**, 566 (1980).
  - [25] N. Troullier and J. L. Martins, *Phys. Rev. B* **43**, 1993 (1991).
  - [26] L. Kleinman and D. M. Bylander, *Phys. Rev. Lett.* **48**, 1425 (1982).
  - [27] O. Sugino and A. Oshiyama, *Phys. Rev. Lett.* **68**, 1858 (1992).
  - [28] S. Saito and S. Okada in *Proceedings of the 3rd Symposium on Atom-Scale Surface and Interface Dynamics* (JSPS-Research-for-the-Future Program, Fukuoka, Japan, 1999), pp. 307–310.
  - [29] R. E. Peierls, *Quantum Theory of Solids* (Clarendon Press, Oxford, 1955) Chap. V.
  - [30] J. W. Mintmire, B. I. Dunlap, and C. T. White, *Phys. Rev. Lett.* **68**, 631 (1992).